Experimental study of the structural and magnetic properties of Fe/Tb multilayers

F. Richomme, J. Teillet, and A. Fnidiki
Laboratoire de Magnetisme et Applications, URA CNRS 808, Faculté des sciences de Rouen, 76821 Mont-Saint-Aignan Cédex, France

P. Auric
Departement de Recherche Fondamentale sur la Matière Condensée Physique, Centre d'Etudes Nucléaires de Grenoble, Boîte Postale 85X, 38041 Grenoble Cédex, France

Ph. Houdy
Université d'Evry, Boulevard des Coquibus, 91025 Evry Cédex, France
(Received 2 August 1995; revised manuscript received 16 January 1996)

Sputtered Fe/Tb multilayers of various Fe and Tb thicknesses ($0.22 \leqslant t_{Fe} \leqslant 3.3$ nm, $0.2 \leqslant t_{Tb} \leqslant 1.9$ nm) have been investigated by x-ray diffraction, Mössbauer spectrometry, and magnetic measurements in the 4.2–300 K temperature range. A compositionally modulated structure is shown with the appearance of pure amorphous iron in the center of the Fe layers thicker than 1.2 nm. When the Fe layers are thick enough ($\geqslant$2.2–2.4 nm), the Fe layers will crystallize. The magnetic properties ($M, T_{comp}, T_c, ...$) were analyzed in relation with Fe and Tb thicknesses and also with mean Tb composition. In agreement with the structure, the departure of magnetic properties from those of the corresponding amorphous alloys is observed when pure amorphous iron appears in the center of the layers. The dependence of the magnetic anisotropy axis on temperature and thicknesses is interpreted taking into account the composition modulation in the multilayers and the dominant magnetic subnetwork. [S0163-1829(96)05725-6]

I. INTRODUCTION

In recent years, materials with an artificial layered structure have attracted considerable attention because of the potential improvements in magneto-optical storage. Many experimental and theoretical investigations have been performed. In particular, many studies have been devoted to rare-earth–transition-metal (RE/TM) multilayers, such as Tb/Fe,[1–9] which can exhibit a strong perpendicular magnetic anisotropy (PMA), a compensation point close to room temperature, and a high coercive field needed for perpendicular magneto-optical recording.

In magnetic RE/TM multilayers, the PMA is mainly attributed to the presence of interfaces and the large magnetocrystalline effect of RE ions.[10,11]

Several experimental studies have been performed to determine the role of interfaces on PMA. In amorphous Tb/Fe multilayers,[1,4] the PMA is found to be stronger for small thicknesses of individual layers. In Nd/bcc Fe multilayers,[12] Mössbauer spectrometry has revealed that the PMA was reinforced when the thickness of the interfaces decreased. In contrast, in the Tb/bcc Fe multilayers studied by Mössbauer spectrometry, a broader alloyed interface is claimed to be responsible for the PMA.[13] Scholz *et al.*[9] showed on Tb/Fe bilayers or trilayers that the Tb/Fe and Fe/Tb interfaces have different magnetic behaviors and that the PMA mainly originated from the Tb/Fe (Tb deposited on Fe) interface, but no structural effect was evidenced in Mössbauer spectra to explain the difference between the two interfaces. Very few investigations using the Mössbauer spectrometry were performed on amorphous Fe/Tb multilayers and the results concerned only one or two samples.[6,14] This is very surprising because the amorphous Fe/Tb multilayers exhibit a strong PMA at room temperature.[11,15]

Here, we report on the structural and magnetic properties of Fe/Tb multilayers using x-ray diffraction (XRD), ^{57}Fe conversion electron Mössbauer spectrometry (CEMS) and magnetization measurements in the 4.2–300 K temperature range. The ^{57}Fe Mössbauer spectrometry is a suitable technique because it gives access directly to the local structure and the direction of magnetic moments of iron. The study will be performed on Fe/Tb multilayers in a wide thickness range in order to determine the different structural and magnetic properties. Previously we have reported on a detailed structural and magnetic diagram obtained by Mössbauer spectrometry at 300 K.[15] Our aim is to correlate the detailed structure of the layers with the magnetic properties. The magnetic anisotropy of the multilayers will be analyzed in detail. The analogies and the differences with the Fe-Tb alloys will be explained.

II. EXPERIMENT

The Tb/Fe multilayer films were deposited at room temperature on commercially available Si (111) substrates using a reactive diode rf-sputtering system with a deposition rate of 0.05 nm s^{-1}. They were chemically etched before insertion into the deposition chamber and covered with a 10-nm-thick Si_3N_4 buffer layer. The Tb/Fe stack always began with an Fe layer and systematically finished with a 10-nm-thick Si_3N_4 top layer to prevent corrosion and oxidation.

The layer thickness and the periodic structure of the film were determined by grazing x-ray reflectometry. The global structure of the films was investigated by high-angle x-ray diffraction using a ⟨⟨INEL CPS 120⟩⟩ curved position-sensitive detector in an evacuated tank. The x-ray generator was equipped with a cobalt anticathode, using $K\alpha$ radiation. Magnetic measurements were determined from SQUID and

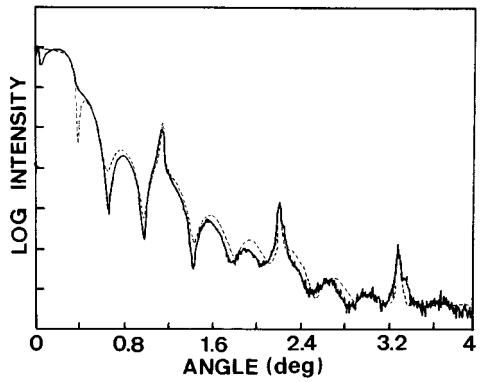

FIG. 1. Grazing x-ray patterns of (2.1 nm Fe/1.9 nm Tb) with 75 bilayers. The solid line is the experimental curve, the dashed line is the fitted curve.

AGFM measurements versus temperature and applied field. The diamagnetic signal of the Si substrate was systematically subtracted. CEMS Mössbauer spectra were recorded using a conventional spectrometer equipped with a homemade helium-methane proportional counter at room temperature and a channeltron detector in the 4.2–300 K temperature range. The source was a ^{57}Co source in a rhodium matrix. The samples were set perpendicular to the incident γ beam. The spectra were fitted with a least-squares technique[16] using the histogram method relative to discrete distributions,[17] constraining the linewidths of each elementary spectrum to be the same (in the case of amorphous spectra). Isomer shifts are given relative to α-Fe at 300 K.

The thickness of terbium layers t_{Tb} varied in the range 0.2–1.9 nm and of iron layers t_{Fe} in the range 0.22–3.3 nm. The samples were deposited with 67–120 periods.

III. X-RAY-DIFFRACTION STUDY

A. Grazing x-ray reflectometry

Some of the samples were checked by grazing x-ray reflectometry (GXR). As an example, the GXR pattern of the (2.1 nm Fe/1.9 nm Tb) amorphous multilayer, reported in Fig. 1, exhibits clearly the three diffraction peaks expected in the angular range studied, evidencing a good layered structure. The estimated period length is in agreement with the value expected from deposition parameters. For samples with crystalline iron layers, the GXR pattern gives all the superstructure peaks expected in the angular range of the measurements (0°–4°).

B. High-angle x-ray diffraction

The experimental pattern for two different series with fixed terbium thickness (t_{Tb}=1.2 and 1.9 nm) and varied iron thicknesses are drawn in Figs. 2 and 3, respectively. Let us consider first the series with t_{Tb}=1.9 nm. At low t_{Fe} (0.22 nm) [Fig. 3(a)] a broad peak typical of an amorphous or nanocrystalline structure is observed, with a maximum intensity for a diffraction angle θ=18°, corresponding to the Tb-Tb interatomic distance (d_{Tb}=0.35 nm).[18,19] The tail of the peak for higher diffraction angles is attributed to an amorphous Tb-Fe interface where the progressive mixing of Fe and Tb atoms produces a progressive decrease of the

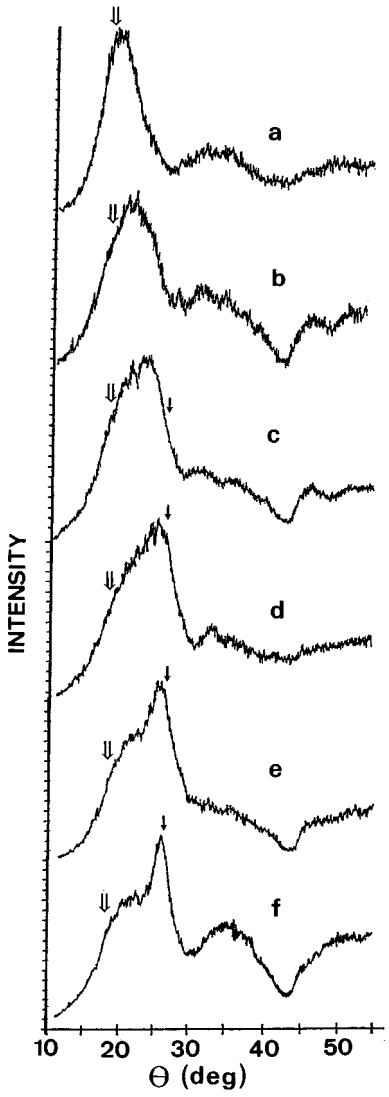

FIG. 2. High-angle x-ray diffraction patterns for multilayers with t_{Tb}=1.2 nm and various values of t_{Fe}: *a*, 0.37 nm; *b*, 0.7 nm; *c*, 1.35 nm; *d*, 1.9 nm; *e*, 2.1 nm; *f*, 2.3 nm. The symbols ⇒, 18°; →, bcc Fe lines.

mean interatomic distance. Increasing t_{Fe} (0.9 nm) [Fig. 3(b)] shifts the main peak to the right and broadens it. The shift means that the mean composition of the interface is higher in iron and that the relative intensity of the interface phase versus the pure terbium phase is increased, i.e., the thickness of the Tb-Fe amorphous interface is increased. The broadening of the peak, when t_{Fe} increases, gives evidence of a composition modulation in the Tb-Fe interface. Next, the peak becomes asymmetrically shaped with the progressive appearance of a pure amorphous iron phase, according to the $d_{\mathrm{Fe\text{-}Fe}}$ length estimated to be 0.250±0.004 nm by several authors.[18–20] This peak, broad at first [Fig. 3(d)], becomes narrower and, simultaneously, higher-order diffraction peaks of iron grow, evidencing a crystallized bcc phase [Fig. 3(e)]. Furthermore, the relative intensities of these lines are in agreement with the results of Pierre *et al.*,[21] who conclude that the (110) iron plane is lying in the layers. Nevertheless, the width of higher-order peaks indicates a slight misorientation. For the iron phase, our interpretation is as follows:

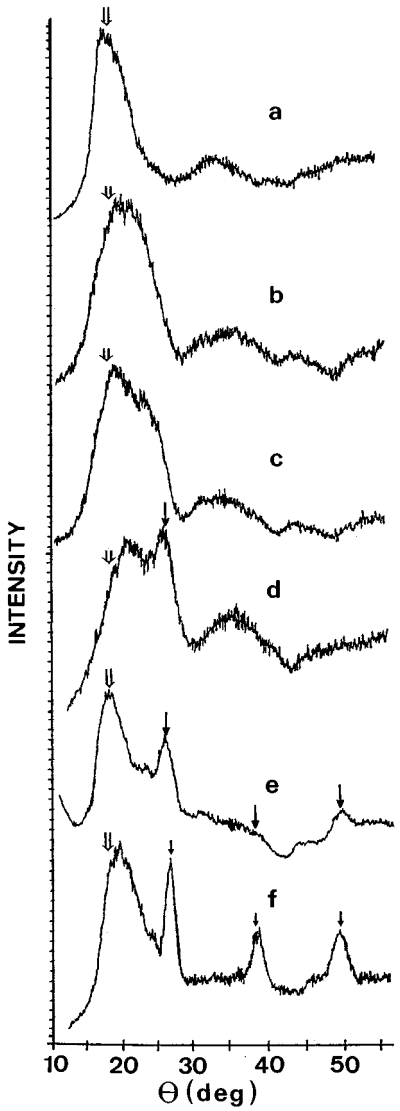

FIG. 3. High-angle x-ray diffraction patterns for the 1.9 nm Tb series with various values of t_{Fe}: *a*, 0.22 nm; *b*, 0.9 nm; *c*, 2.1 nm; *d*, 2.35 nm; *e*, 2.7 nm; *f*, 3.3 nm. (⇒, 18°; →, bcc Fe lines).

pure amorphous or nanocrystalline iron appears in the middle of the ''iron layers'' when the thickness of this amorphous iron is large enough, higher than a critical thickness. This is clearly observed from $t_{Fe}=2.1$ nm. Then, the pure iron crystallizes, probably following a nucleation-growth process. This result is in agreement with *in situ* kinetic ellipsometry measurements.[21] With the appearance of pure crystalline iron, a narrowing of the first broad peak is observed. The interface seems to be poorer in iron. This behavior looks like the segregation observed in a demixing process. Such behavior has already been reported when iron crystallizes in amorphous Tb-Fe alloys, by Krishnan and Machizaud.[22] Further experiments showed that the nanosegregation is produced by the nucleation and growth of the stable Fe-rich amorphous phase. When this phase crystallizes, then Tb in excess is ejected.[23] So, such a mechanism should be enhanced by the alternating deposition of Fe and Tb occurring in multilayers.

For series with $t_{Tb}=1.0$ nm and $t_{Tb}=1.2$ nm (Fig. 2), the evolution of the pattern with t_{Fe} is similar to what was observed for $t_{Tb}=1.9$ nm. Nevertheless, the first peak is shifted right, showing that pure amorphous terbium, which would be located at $\theta=18°$, does not exist or is negligible. For these terbium thicknesses, we will probably only have a compositionally modulated amorphous Fe-Tb interface and, when t_{Fe} is sufficient, a pure Fe phase in the center of the iron layers will appear.

Pure amorphous iron is clearly observed from 1.7 nm when $t_{Tb}=1.0$ nm, 1.9 nm when $t_{Tb}=1.2$ nm, and 2.1 nm when $t_{Tb}=1.9$ nm. Taking into account the sensitivity of this technique means that it actually appears at thinner thicknesses. For example, assuming that pure amorphous Fe appears from 1.2 nm when $t_{Tb}=1.0$ nm, as we will see later, it means that it would be experimentally observed from about two monolayers. The value seems to increase with t_{Tb}, but, due to the experimental uncertainties, no definitive conclusion can be made on the dependence of the pure iron appearance threshold with t_{Tb}. However, the iron thickness needed for crystallization of pure iron increases slightly with t_{Tb}. It is estimated at 2.3 nm for $t_{Tb}=1.2$ nm and between 2.4 and 2.7 nm for $t_{Tb}=1.9$ nm. There is no reason for this dependence not to work for the appearance of pure amorphous iron. These crystallization thicknesses are in rough agreement with most other studies on sputtered or evaporated Tb/Fe multilayers.[2,3,6,24] It is noteworthy that few authors found smaller values [0.8 nm,[25] 1.0 nm,[26,27] 1.5 nm (Ref. 28)], but, in these cases, the terbium layer was in the 1–2 monolayer range.

Here, assuming that pure amorphous iron appears from 1.2 nm, the Tb/Fe or Fe/Tb interface would spread on a thickness close to 1.2 nm, i.e. about 2(Tb+Fe) monolayers ($d_{Fe}=0.25$ nm, $d_{Tb}=0.35$ nm). So, an interdiffusion of terbium and iron atoms takes place, probably related mainly to the defects in the interface (vacancies, surface steps, etc.). According to the different iron and terbium atomic radii, such an interdiffusion process should lead to different Tb on Fe and Fe on Tb interfaces, the Fe on Tb interface being thicker. This is what was observed by Richomme *et al.* using ^{57}Fe Mössbauer spectrometry for multilayers with crystallized iron, but, surprisingly, not for multilayers with amorphous iron.[29]

IV. ^{57}Fe MÖSSBAUER STUDY

Most of the results at room temperature have already been previously published.[15] The t_{Tb}-t_{Fe} diagram (Fig. 4) summarizes our structural and magnetic results on the *iron layers*. For $t_{Tb}>0.35$ nm (one terbium monolayer), the iron layers are amorphous up to an iron thickness, which, in agreement with x-ray studies, increases slightly with t_{Tb} (2.3 nm for $t_{Tb}=1.2$ nm, 2.4–2.7 nm for $t_{Tb}=1.9$ nm). They then crystallize, the remaining amorphous part being attributed to the Tb-Fe interface. Fitting of spectra agrees with 2 iron monolayers involved in each interface. The magnetic anisotropy, which at first is perpendicular, rotates towards the basal plane from $t_{Fe}\sim1.5$ nm. The rotation is achieved at about 2.0 nm. According to the x-ray studies, this rotation is correlated with the appearance and the thickening of the pure amorphous iron at the center of the iron layers.

The temperature dependence of Mössbauer spectra is reported in the amorphous range for three typical iron thick-

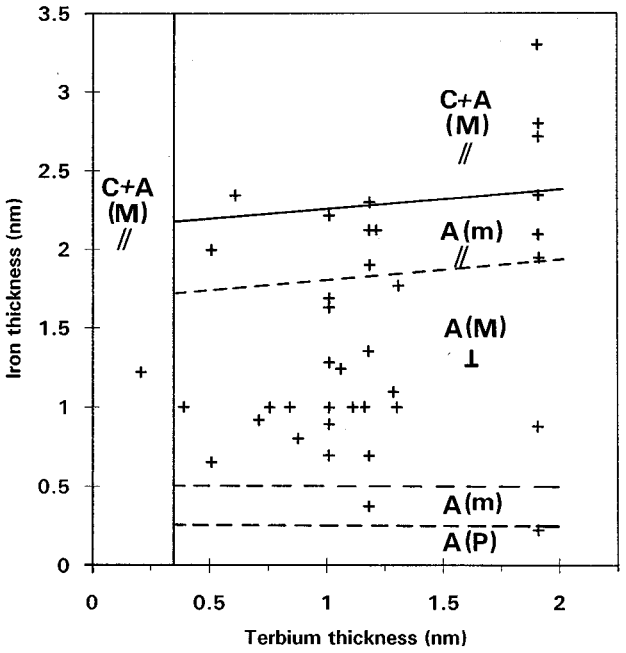

FIG. 4. (t_{Tb},t_{Fe}) Mössbauer diagram of structural and magnetic properties of Fe/Tb multilayers at 300 K. The symbols *C*, crystal; *A*, amorphous; *M*, magnetic; *m*, weakly magnetic; *P*, paramagnetic; ∥, parallel magnetic anisotropy; ⊥, perpendicular magnetic anisotropy. The lines are only indicated as a guide for the eyes.

nesses: 1.3 nm Fe/1.0 nm Tb [Fig. 5(a)], 1.7 nm Fe/1.0 nm Tb [Fig. 5(b)], 2.1 nm Fe/1.9 nm Tb [Fig. 5(c)]. The spectra are characteristic of an amorphous structure and their shape strongly depends on temperature. Because of their asymmetry and their broadening which are related to the distribution of Tb and Fe environments, they were fitted with a linearly correlated distribution of both isomer shift (IS) and hyperfine field. Let us discuss the shape of the hyperfine field distribution $P(B_{hf})$ at room temperature. For $t_{Fe}=1.3$ nm, it is very similar to what is observed in Tb-Fe alloys of the same global composition, indicating that such a multilayer behaves as an alloy: this is in agreement with the compositionally modulated structure. This is confirmed by the $\langle IS \rangle$ values (≈ -0.10 mm/s). For $t_{Fe}=1.7$ nm, $P(B_{hf})$ shows two components: the higher field component, which is analogous to the above-mentioned sample, is attributed to the compositionally modulated interface. The lower component, located at low field (<5 T), is assumed to be due to the pure amorphous iron at the center of the iron layers. When t_{Fe} increases (2.1 nm), the contribution at low field is increased, in accordance with the increasing of the pure amorphous iron part. For $t_{Fe}=2.1$ nm and $t_{Fe}=1.7$ nm, the mean hyperfine field is much lower than that observed in corresponding Fe-Tb alloys. The amorphous iron is thought to be paramagnetic above $T_c \sim 200$ K,[30,31] and the low component could be due mainly to quadrupolar effects related to structural effects in this paramagnetic phase (the overall splitting due to a field of 3 T is of the order of a quadrupolar splitting of 1 mm/s). Probably, some neighboring magnetic effects will also contribute to $P(B_{hf})$. The amorphous iron, paramagnetic at 300 K, seems to appear above 1.5 nm of Fe, which means that the pure amorphous iron appears at a thinner t_{Fe}. Indeed, the observed nonmagnetic iron corresponds to the part of pure

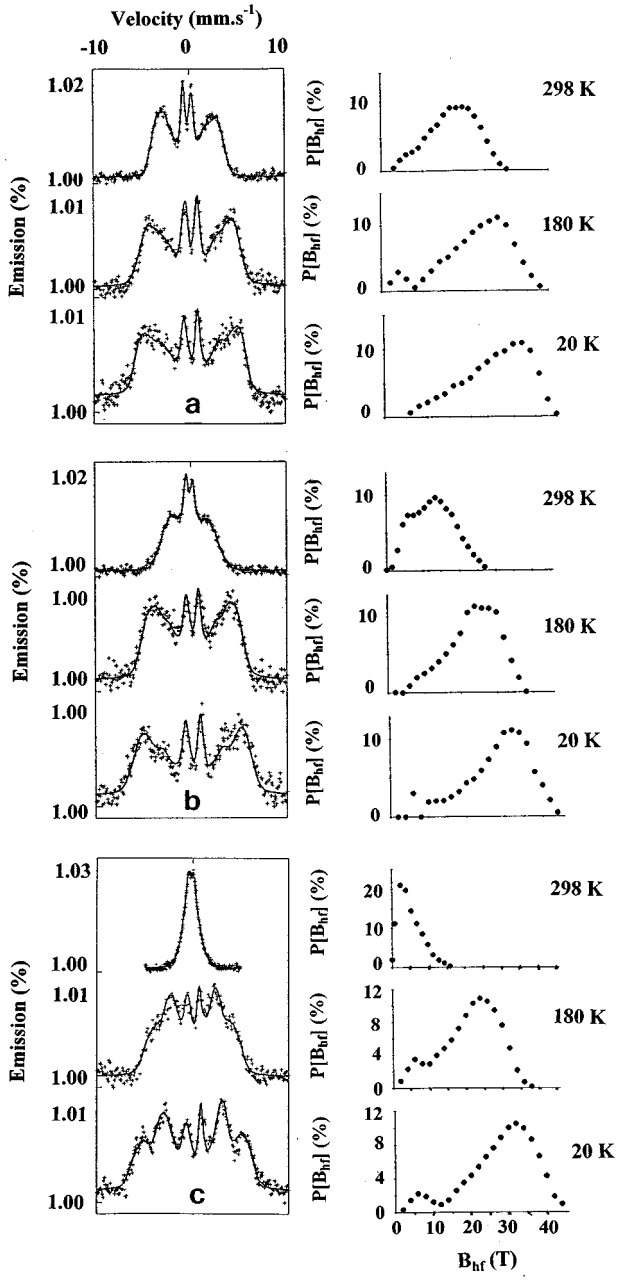

FIG. 5. CEMS spectra and their corresponding hyperfine field distributions for some Fe/Tb multilayers at 298, 180, and 20 K: (a) 1.3 nm Fe/1.0 nm Tb; (b) 1.7 nm Fe/1.0 nm Tb; (c) 2.1 nm Fe/1.9 nm Tb.

amorphous iron which is not disturbed by the magnetic Fe-Tb interfaces, i.e., which is outside the magnetic correlation zone. At 180 K, $P(B_{hf})$ curves show unambiguously that all the phases are magnetic. At 20 K, the $P(B_{hf})$ spreads up to 45 T, for $t_{Fe}=1.7$ and 2.1 nm, which is much higher than the value found in bcc Fe (34.3 T) at 4.2 K, and is probably due to the amorphous iron structure (interatomic Fe-Fe distance and coordination number).

The fitted Mössbauer parameters are reported in Table I for the whole range of iron thicknesses, including one sample with crystallized iron. In the amorphous range, at constant $t_{Tb}=1.0$ nm, the dependence on the iron thickness of the mean hyperfine field at the iron site at 20 and 300 K is shown in Fig. 6. For $t_{Fe} \geq 1.5$ nm, $\langle B_{hf} \rangle$ reaches a maximum

TABLE I. Fitted Mössbauer parameters for sputtered Fe/Tb multilayers. t_{Fe} and t_{Tb} are, respectively, the nominal Fe and Tb thicknesses, X is the mean atomic Tb composition, T is the temperature, $\langle IS\rangle$ is the mean isomer shift, $\langle B_{hf}\rangle$ is the mean hyperfine field, β the mean Mössbauer angle, and an asterisk means that the iron layer is crystallized.

Fe/Tb multilayers							Fe-Tb alloys (Refs. 32 and 38)
t_{Fe} (nm)	t_{Tb} (nm)	X (at. % Tb)	T (K)	$\langle IS\rangle$ (mm/s)	$\langle B_{hf}\rangle$ (T)	β (°)	$\langle B_{hf}\rangle$ (T)
0.9	1.0	29.0	300	−0.10	15.4	33	17.0
			180		20.6	33	
			20		22.8	33	
1.3	1.0	22.1	300	−0.10	15.6	10	18.5
			180		23.0	23	
			20		25.3	27	
1.7	1.0	17.7	300	−0.08	11.3	20	17.2
			180		23.0	29	
			20		28.2	30	
2.2	1.0	14.0	300	−0.06	1.9	84	11.7
			180		19.3	45	
			20		27.2	45	
2.1	1.9	24.8	300	−0.08	4.9	74	18.2
			180		21.1	59	
			20		27.7	61	
3.3*	1.9	4.8	300	−0.002	28.9	90	
			180		31.2	70	
			20		32.5	63	

value of 28 T and remains nearly constant at 20 K, while it dramatically decreases at room temperature, at a much faster rate than Fe-Tb alloys with the same mean composition.[32] At 20 K, the increase of $\langle B_{hf}\rangle$ with t_{Fe} is related to the increasing number of iron neighbors at a given iron site.

The temperature dependence of the mean hyperfine field (Fig. 7) allows us to estimate the Curie temperatures (Table II), which are found to be lower than those of amorphous Fe-Tb alloys of same composition (cf. Sec. V B).[33,34] It has been suggested that the decrease of the mean hyperfine field at room temperature could be due to a change in the microstructural iron layers, a grain size effect or an appearance of multidomain grains.[6,27,35] We show that the decrease is, in fact, due to an effect of Curie temperature in multilayers, larger than in the corresponding amorphous alloys. This effect will be explained in Sec. V B.

The greater mean hyperfine field at 0 K is related to the lower Curie temperature, in agreement with appearance and increasing of pure amorphous iron in the center of the Fe layers. The effect of amorphous iron can also be evidenced from the normalized curve $B_{hf}(T)/B_{hf}(0)=f(T/T_c)$ (Fig. 8), which exhibits, when t_{Fe} increases, a flattening related to fluctuations of magnetic exchange integrals,[36] due to the increase of the composition gradient.

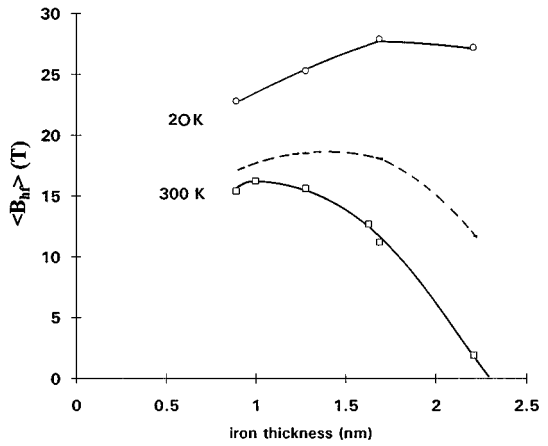

FIG. 6. Mean hyperfine field $\langle B_{hf}\rangle$ as a function of iron thickness (t_{Fe}) at 20 and 300 K. Solid line, Fe/Tb multilayers with t_{Tb}=1.0 nm; dashed line, Fe-Tb amorphous alloys at 300 K (Ref. 32). [The iron thicknesses corresponding to the mean atomic Tb composition were calculated using relation (1).]

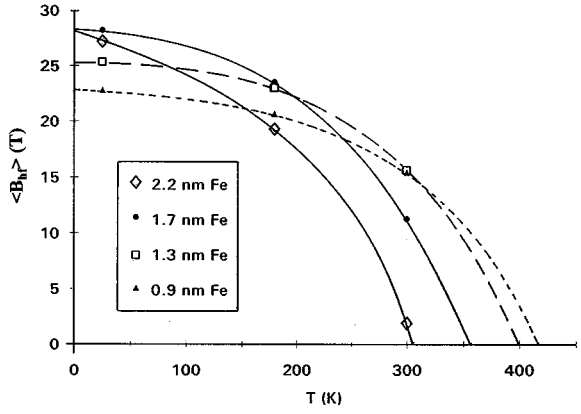

FIG. 7. Temperature dependence of the mean hyperfine field $\langle B_{hf}\rangle$ for some Fe/Tb multilayers with 1.0 nm Tb.

TABLE II. Curie temperatures of amorphous Fe/Tb multilayers deduced from Mössbauer and magnetization measurements.

t_{Fe} (nm)	t_{Tb} (nm)	X (at. % Tb)	T_c (K)
0.9	1.0	29.0	420
1.3	1.0	22.1	400
1.7	1.0	17.7	355
2.2	1.0	14.0	320
0.9	1.9	44.0	415
1.95	1.9	26.2	340
2.1	1.9	24.8	325
2.35	1.9	22.7	315

V. MAGNETIC STUDY

This study was performed for the two previous $t_{Tb}=1.0$ and 1.9 nm series in the temperature range 4.2–300 K and the magnetic field range 0–1.8 T, limited to the amorphous samples.

The results will be interpreted in relation to t_{Fe} and t_{Tb}, but also in relation with the mean atomic Tb composition of the multilayer, noted X, in order to compare these results more easily with the results of corresponding Fe-Tb amorphous alloys.

The mean atomic Tb composition X of the multilayer can be defined from the as-deposited t_{Tb} and t_{Fe} thicknesses taking into account the atomic volumes of Tb and Fe atoms:

$$X=\frac{N_{Tb}}{N_{Tb}+N_{Fe}}=\frac{t_{Tb}/V_{Tb}}{t_{Tb}/V_{Tb}+t_{Fe}/V_{Fe}}$$

$$=\frac{1}{1+(d_{Tb}/d_{Fe})^3(t_{Fe}/t_{Tb})}, \quad (1)$$

where N_{Tb} (N_{Fe}) is the number of Tb (Fe) atoms, V_{Tb} (V_{Fe}) is the atomic volume of Tb (Fe), d_{Tb} (d_{Fe}) is the atomic diameter of Tb (Fe) with $d_{Tb}=0.35$ nm and $d_{Fe}=0.25$ nm.[18–20]

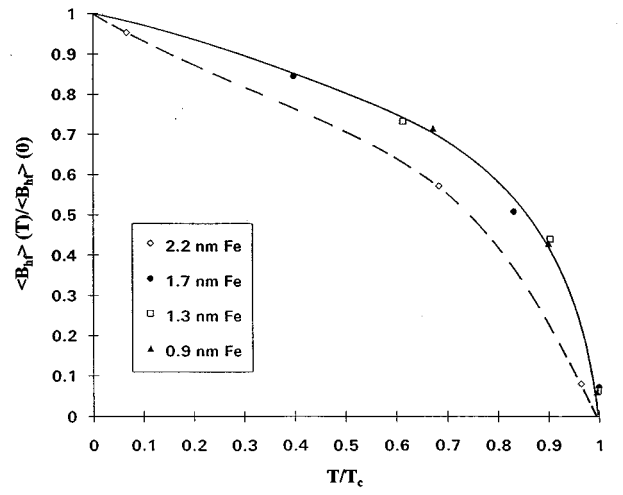

FIG. 8. Normalized curves of the mean hyperfine field vs temperature for various iron thicknesses ($t_{Tb}=1.0$ nm).

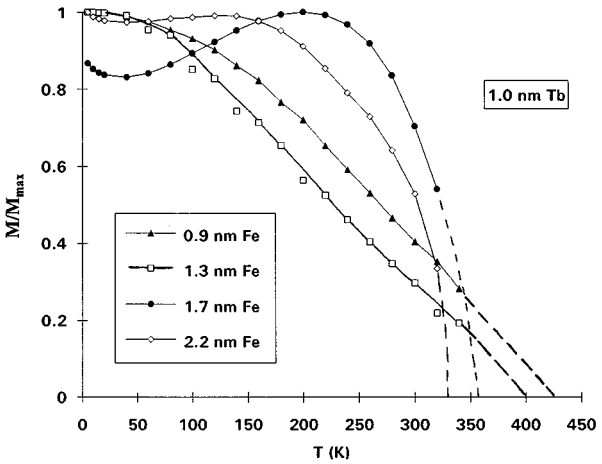

FIG. 9. Reduced magnetization curves M/M_{max} vs temperature for some samples of the $t_{Tb}=1.0$ nm series.

A. Magnetization versus temperature

The temperature dependence of the magnetization for a magnetic field of 1 T applied perpendicularly to the layers is reported in Fig. 9 for the $t_{Tb}=1.0$ nm series.

For $t_{Fe}<1.5$ nm ($X>0.19$), we showed that the multilayer is essentially made up of a compositionally modulated alloy, where Tb and Fe moments are ferrimagnetically coupled. The rare-earth sublattice dominates at all temperatures for $t_{Fe}=0.9$ or 1.3 nm, but for $t_{Fe}=1.7$ nm, this sublattice dominates only at low temperatures and the iron sublattice dominates at higher temperatures. The compensation temperature defined by the minimum of the curve seems to be around 30 K. This minimum does not vanish to zero because of the effects related to the applied field and to composition inhomogeneities.

For $t_{Fe}=2.2$ nm ($X=0.14$), the multilayer is made up of a compositionally modulated interface and a pure amorphous iron phase in the center of the iron layers. So the interpretation of the magnetization curve is more difficult, because we need to take into account several magnetic zones inside the Fe/Tb multilayer at low temperature: a ferrimagnetically coupled Tb/Fe interface, a ferromagnetically coupled iron phase, and exchange interactions between these two phases. It can be assumed that, according to the previous result for $t_{Fe}=1.7$ nm, Tb is still magnetically dominant in the interface, but the pure amorphous iron phase, ferrimagnetically coupled to this interface, will enhance the iron subnetwork. Here, we will show later that the Fe sublattice dominates at all temperatures despite the observed flat minimum, which is probably an artefact related to the two phases.

For $t_{Tb}=1.9$ nm and $t_{Fe}<1.5$ nm, the multilayers are composed at low temperature of two magnetic zones: compositionally modulated interface with Tb dominant and pure Tb phase. So the RE sublattice would dominate at all temperatures. When t_{Fe} thickness is sufficient to provide a third magnetic zone, i.e., a pure amorphous iron ferromagnetic phase (from $t_{Fe}=1.5$ nm), this phase is coupled ferrimagnetically to the interface. At high temperatures, pure amorphous iron and terbium phases are no longer magnetic, but the iron sublattice could dominate in the interface, due to the decrease of

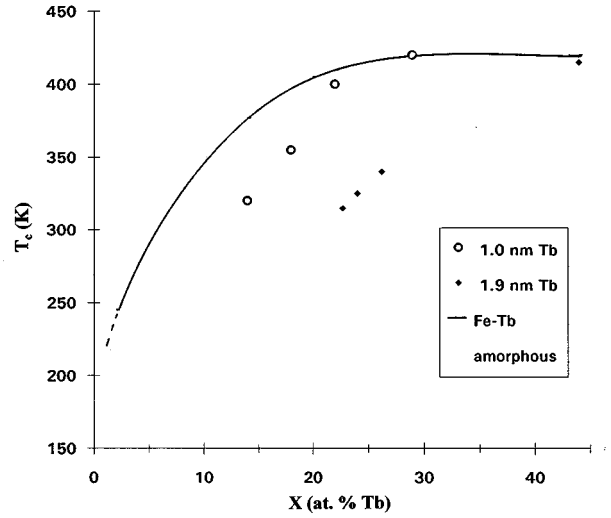

FIG. 10. Curie temperature T_c as a function of terbium atomic fraction X for Fe-Tb amorphous alloys and some Fe/Tb multilayers of the 1.0 and 1.9 nm Tb series.

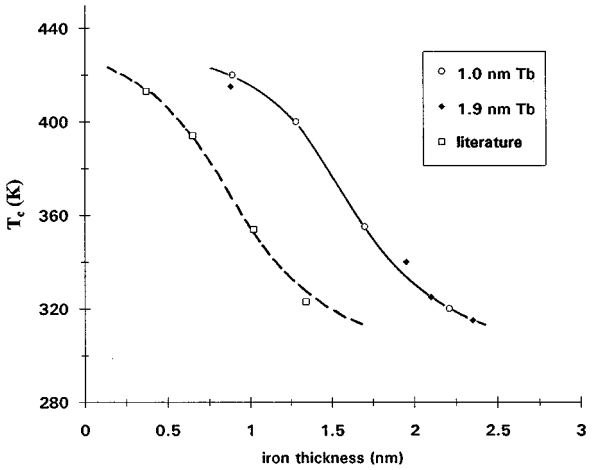

FIG. 11. Dependence of Curie temperatures T_c on t_{Fe}. Solid line, our results for the $t_{Tb}=1.0$ and 1.9 nm series; dashed line, our curve translated towards lower values of t_{Fe}; (□), experimental results for Fe/Tb multilayers from Honda *et al.* (Ref. 5).

terbium moments. The complexity of the exchange inside the layers does not allow an interpretation of the curves in terms of a dominant sublattice.

The extrapolated T_c, which are in agreement with the values deduced from Mössbauer measurements, are reported in Table II.

B. Curie temperature of amorphous multilayers

In the thickness range where no crystalline iron is evidenced, the experimental Curie temperatures of multilayers can be compared to those of the amorphous Tb-Fe films in order to characterize the influence of the multilayered structure, especially of the t_{Tb} and t_{Fe} thicknesses.

The calculated X values are reported in Table II and the X dependence of T_c is reported in Fig. 10, both for multilayers and for amorphous Fe-Tb films.[33,34] Both curves show that the T_c value depends not only on X (i.e., the t_{Tb}/t_{Fe} ratio), but also on t_{Tb} and t_{Fe} independently.

For high X values, T_c seems to be similar to what is observed in amorphous alloys. Down to a threshold value $X=X_S$, T_c departs from the value of alloys and decreases faster. This result is consistent with previous results. Let us consider first the $t_{Tb}=1.0$ nm series. For $X>X_S$, the ML is only composed of a compositionally modulated alloy, for which T_c is very close to the T_c of amorphous alloys. For $X<X_S$, the appearance of pure amorphous iron ($T_c=200$ K) is responsible for the faster decrease of T_c. Experimental results suggest there will be a roughly linear decrease. With this assumption, the intersect with the alloys curve provides $X_S=0.24$ and, consequently $t_{Fe}=1.2$ nm. This could provide a true value for the appearance of pure amorphous iron. In fact, it is the value for which the departure is observed and for which the alloy model is no longer valid. The departure could also start when the modulation becomes too high, leading to a slightly higher t_{Fe} value for the appearance of pure amorphous iron. Nevertheless, a linear decrease of T_c would suggest that the first assumption is correct. It is noteworthy that the linear extrapolation would give T_c close to 200 K at $X=0$, in agreement with estimated T_c values of pure amorphous iron. Let us now consider the $t_{Tb}=1.9$ nm series. Using again the linear assumption gives $X_S=0.37$ from Fig. 10 and, so, $t_{Fe}=1.2$ nm; this value is in remarkable agreement with the previous value, showing once more that the departure is mainly due to the pure amorphous Fe phase.

This confirms that the threshold value is lower than what was deduced from x-ray diffraction (~1.7 nm) and Mössbauer spectrometry (~1.5 nm). This could be related to the sensitivity of these two techniques.

The dependence of T_c on t_{Fe} is reported in Fig. 11. It is clearly seen that it depends strongly on t_{Fe}, but not (or very few) of t_{Tb}. It means that the pure amorphous terbium phase has little influence on T_c. This is probably due to the magnetic properties of this phase and we have no definitive conclusion on this result. In Fig. 11, we have also reported results of Honda *et al.*[5] on sputtered samples with the t_{Fe}/t_{Tb} ratio fixed at 0.5. It is striking to observe a similar behavior, but with a global translation of 0.6 nm towards lower values of t_{Fe}. This translation agrees with different experimental results for crystallization of iron: they found that this crystallization occurs from 1.7 nm in their samples, in place of 2.2–2.4 nm in our samples. So the difference seems to be related only to the interfaces, which are probably smoother in our samples.

C. Magnetization versus X

At room temperature, the data were obtained with a field of 1.0 or 1.8 T applied parallel or perpendicular to the layers. For the lower field, the results are still slightly dependent on the orientation of the field, but not for the higher field. If we report the results for the whole set of samples versus X, no straightforward evolution can be deduced, indicating that, as already observed for the Curie temperature, the results are also dependent on the multilayer structure, i.e., of t_{Tb} and t_{Fe} separately. Consequently, we will study separately three series, either at fixed t_{Tb} and varied t_{Fe} ($t_{Tb}=1.0$ and 1.9 nm) or at fixed t_{Fe} and varied t_{Tb} ($t_{Fe}=1.0$ nm). The three series are studied in relation to t_{Fe}, t_{Tb} (Fig. 12), and X (Fig. 13).

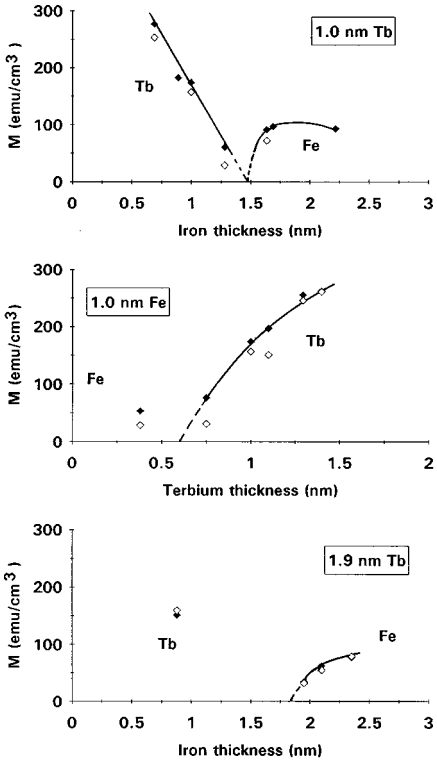

FIG. 12. Magnetization curves vs individual thicknesses for the 1.0 nm Tb (varied t_{Fe}), 1.0 nm Fe (varied t_{Tb}), and 1.9 nm Tb series. The magnetic field (1.0 T) was applied perpendicular to (♦) and parallel to (◇) the film plane. The dominant sublattices are reported in the figure.

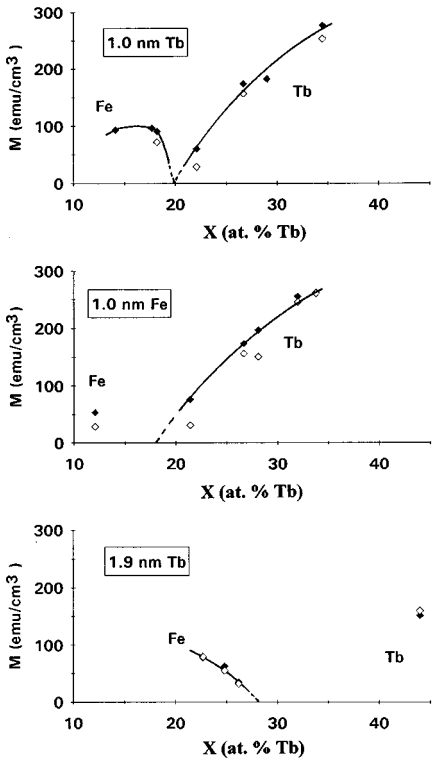

FIG. 13. Magnetization curves vs X for the 1.0 nm Tb (varied t_{Fe}), 1.0 nm Fe (varied t_{Tb}), and 1.9 nm Tb series. The magnetic field (1.0 T) was applied perpendicular to (♦) and parallel to (◇) the film plane. The dominant sublattices are reported in the figure.

The curves give evidence of a compensation composition X_{comp} (T_{comp}=300 K), indicating the change of the dominant sublattice at room temperature. X_{comp} is found to be not dependent on the applied field (1.0 or 1.8 T) and the experimental values of X_{comp} and associated t_{Fe} and t_{Tb} (calculated using relation 1) are reported in Table III. It is seen that X_{comp} depends on t_{Tb} and t_{Fe} separately. X_{comp} is not found to be the same as those of corresponding Fe-Tb amorphous alloys. Its variation is probably complex, depending on the thickness of the interface between layers, i.e., on the roughness of the multilayers.

It is noteworthy that the three X_{comp} values (corresponding to the same T_{comp}=300 K) correspond to three multilayers with three different T_c, the higher X_{comp} corresponding to the lower T_c. For amorphous alloys, T_{comp}=300 K for X_{comp}=0.22,[33,34,37] which is somewhat surprising, because we would expect the lowest value for alloys (highest T_c).

For the t_{Tb}=1.0 nm series, measurements were also performed at 10 K (Fig. 14). As observed in amorphous alloys, X_{comp} decreases with the temperature according to the higher temperature dependence of the rare-earth magnetization. The change of the dominant subnetwork with the temperature is confirmed for the sample (1.7 nm Fe/1.0 nm Tb, X=0.177) in good agreement with the $M(T)$ curve, which exhibits a T_{comp} higher than 10 K. Examination of the two curves $M(X)$ at 10 and 300 K confirms that the small decrease observed on the $M(T)$ curve for t_{Fe}=2.2 nm (X=0.14) is not due to a compensation point.

The decrease of M observed on the experimental curve at room temperature for $X<0.17$ is correlated to the low values of the Curie temperatures which are close to room temperature, due to the pure amorphous iron at the center of the Fe layers.

VI. MAGNETIC ANISOTROPY

A. X dependence at room temperature

This dependence will be visualized from magnetization M (see above), the coercive field H_c deduced from hysteresis loops, which will be published elsewhere and from the Mössbauer β angle, which is deduced from the relative intensities of the Mössbauer lines and which is a measurement of the mean angle of the hyperfine field with the γ-ray direction, i.e., with the normal to the layers.

Let us recall that the Mössbauer spectrum is fitted as a distribution of elementary sextets with relative line intensities 3,y,1,1,y,3 for a sextet. The β angle is given by the relation $y=4\sin^2\beta/(2-\sin^2\beta)$. Here, the β value was con-

TABLE III. Data concerning the compensation point in Fe/Tb multilayers at 300 K.

t_{Fe} (nm)	t_{Tb} (nm)	X_{comp} (at. % Tb)	$t_{Fe\ comp}$ (nm)	$t_{Tb\ comp}$ (nm)
Varying	1.0	19.7	1.5	1.0
Varying	1.9	28.0	1.8	1.9
1.0	Varying	18.0	1.0	0.6

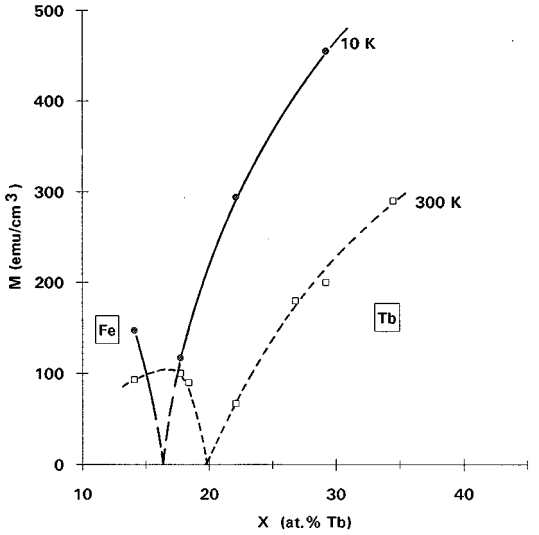

FIG. 14. X dependence of the magnetization M for some samples of the 1.0 nm Tb series at 10 and 300 K. The magnetic field (1.0 T) was applied perpendicular to the plane.

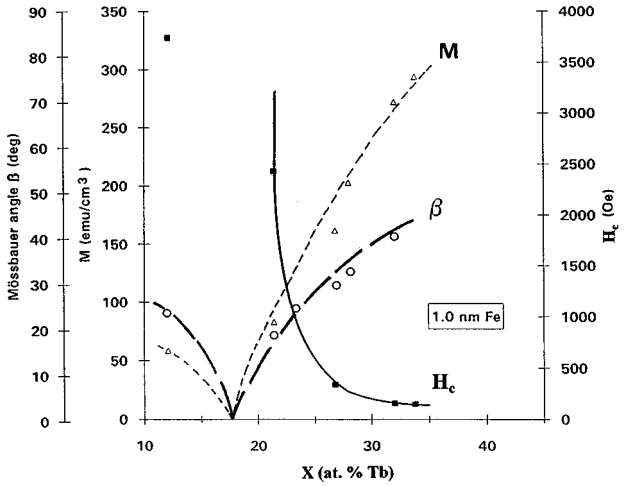

FIG. 16. X dependence of the magnetization M, the coercive field H_c, and the mean Mössbauer β angle for multilayers of the constant 1.0 nm Fe series at 300 K. The lines are indicated only as guides to the eye.

strained to be the same for all the elementary sextets and the fitted value is thus an averaged value of the direction of iron moments. In a few Mössbauer spectra, overlapping of lines occurs, leading to less accurate fitted β values. In such cases, a systematic study of the shape of $P(B_{\mathrm{hf}})$ versus the β value allows us to determine this value accurately. It is noteworthy that β is measured in a zero applied field, while M and H_c need an applied magnetic field.

The X dependence of these quantities is reported in Fig. 15 for the constant 1.0 nm t_{Tb} series and in Fig. 16 for the constant 1.0 nm t_{Fe} series. Let us discuss first the $t_{\mathrm{Tb}}=1.0$ nm series. As usual, H_c exhibits a strong maximum at the compensation composition X_{comp} defined by $M=0$. Indeed, the demagnetizing field, proportional to the magnetization, vanishes. The extrapolated β value is thus zero, indicating a perfect perpendicular anisotropy, related to the interface anisotropy and the Tb-Fe ferrimagnetic exchange coupling. It is noteworthy that the PMA in multilayers appears to be stronger than in amorphous Fe-Tb alloys where the minimum Mössbauer angle is 20°.[32,38]

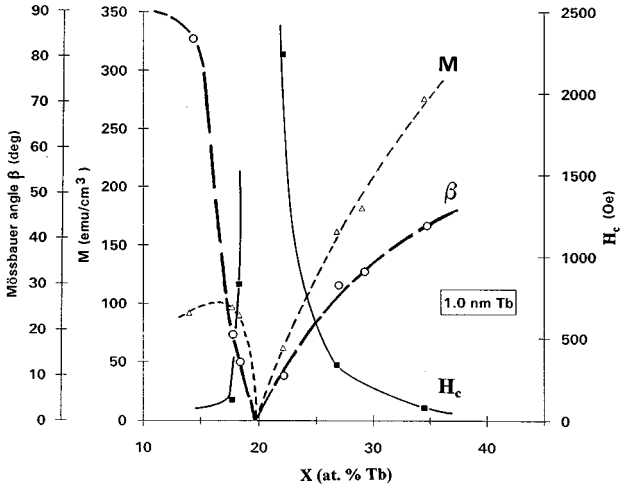

FIG. 15. X dependence of the magnetization M, the coercive field H_c, and the mean Mössbauer β angle for multilayers of the constant 1.0 nm Tb series at 300 K. The lines are only guides to the eye.

For X higher than X_{comp} ($t_{\mathrm{Fe}}<1.5$ nm), the increase of β evidences for a rotation of the direction of the iron moments. This increase is very similar to that of magnetization. So, the demagnetizing field will progressively increase, leading to the progressive rotation of moments towards the layer plane and it is expected that β will tend towards 90° for higher X values. The iron layers are getting thinner. They do not contain pure iron and become richer in terbium atoms. It can be assumed that, for sufficiently thin iron layers, pure nonmagnetic amorphous terbium will appear in the center of the Tb layers. This appearance of nonmagnetic layers will isolate the different layers and so could reduce magnetic interactions between them, enforcing planar anisotropy. This is in agreement with what was suggested to explain the variation of anisotropy with RE thickness in RE/bcc Fe (RE=Pr, Nd, Tb) crystalline multilayers by Mibu *et al.*[39] Nevertheless, this is only an assumption for this part of the curve because the samples studied ($0.29\leqslant X\leqslant 0.35$) only contain a compositionnally modulated phase and the experimental β values are similar to what was observed in corresponding amorphous alloys.

Below X_{comp}, the iron sublattice dominates magnetically. t_{Fe} increases, the iron layers become poorer in terbium atoms and nonmagnetic pure amorphous iron layers, present from $t_{\mathrm{Fe}}=1.2$ nm, will grow. For this part of the curve, M increases first. The explanation is similar to that given above and, when M increases, the demagnetizing field, which forces the iron moments to lie in the planes ($\beta=90°$), contributes to the rotation of iron moments from the perpendicular direction. Then, for $X<0.17$ ($t_{\mathrm{Fe}}>1.8$ nm), when nonmagnetic pure amorphous iron is thick enough, M decreases because of the decrease of T_c close to room temperature (see Sec. V C). Nevertheless, β continues to increase faster than in corresponding amorphous Tb-Fe alloys [for $X=0.14$,

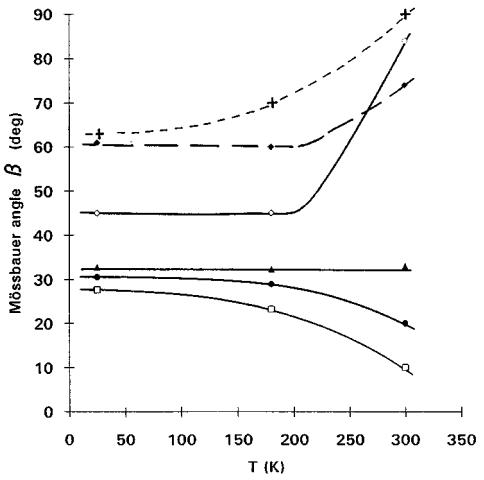

FIG. 17. Temperature dependence of the fitted mean Mössbauer β angle for some multilayers of the 1.0 nm Tb series {▲, 0.9 nm Fe; □, 1.3 nm Fe; ●, 1.7 nm Fe; ◇, 2.2 nm Fe} and of the 1.9 nm Tb series {◆, 2.1 nm Fe; +, 2.7 nm Fe}.

β(ML)=85°$\gg\beta$(alloy)=23° (Refs. 32 and 38)]. This could be explained by the reduction of interactions related to nonmagnetic layers.

For t_{Fe}=1.0 nm series (Fig. 16), experimental results are scarcer and the experimental β curve below X=0.20 is less accurate. For example, it cannot be concluded that the β angle at the compensation point is zero, but only that it is less than 20°. Nevertheless, extrapolated variation curves are in agreement with the previous explanation and are probably close to the true experimental values. Above X_{comp} (t_{Tb}>0.6 nm), the curves of M and β are similar to those observed for the t_{Tb}=1.0 nm series. Below X_{comp}, the experimental point (1.0 nm Fe/0.38 nm Tb, X=0.12) exhibits a β angle value (β=24 °) lower than the multilayer of the same composition in the 1.0 nm Tb series (2.2 nm Fe/1.0 nm Tb, X=0.14, β=84 °). The difference is probably due to a different layered structure related to the thinner thickness of terbium. Indeed, the sample of this series exhibits a higher T_c which means that the thickness of pure amorphous iron is thinner (for 0.38 nm of Tb the estimated pure iron thickness is 0.7 nm instead of 1.2 nm for 1.0 nm of Tb). The pure amorphous iron is not sufficient to greatly reduce the interlayer coupling.

B. Temperature dependence

In Fig. 17 is reported the temperature dependence of the fitted Mössbauer β angles for some samples of 1.0- and 1.9-nm fixed terbium series. Let us first discuss the 1.0-nm Tb series.

At low temperature (20 K) and for $t_{Fe}\leqslant$1.7 nm, the β value is close to 30°. As previously seen, terbium atoms are magnetically dominant. Pure amorphous iron or terbium phases are absent or negligible. Tb is a non-S state rare earth with a strong spin-orbit coupling, giving rise to single-ion anisotropy. In RE-Fe amorphous materials, this magnetic anisotropy is randomly distributed because of the structural disorder [random magnetic anisotropy (RMA)].[40,41] So, the misorientation of iron moments (β=30°) at low temperature can be attributed, via the Tb-Fe ferrimagnetic coupling, to the enhancement of the random distributed terbium magnetic moments in the interface. The β value is intermediary between the RMA value (54,7°) and the perpendicular interface anisotropy value (0°). This behavior is in agreement with predictions of a model developed by Dieny *et al.*,[42] where a strong pinning of spacially distributed RE moments is observed for a large anisotropy, when RE magnetization is dominant. For these multilayers, the β values at 300 K were explained in the Sec. VI A and the evolution of the β angles is progressive between 20 and 300 K.

At 20 K, for t_{Fe}=2.2 nm, the iron subnetwork contains an amount of pure amorphous iron, which is now magnetic, and dominates at low temperature. So, the competition between the PMA of interfaces, the RMA of terbium at the interfaces and the planar anisotropy of the pure iron part provides an intermediate value (~45°). The variation of β with temperature is more peculiar. It remains constant up to 200 K, in a temperature range where pure iron is supposed to be magnetic.

At 20 K, the higher β value for t_{Tb}=1.9 nm and t_{Fe}=2.1 nm compared to that for the (2.2 nm Fe/1.0 nm Tb) sample is assumed to be due to pure amorphous terbium, which is magnetic at low temperature and which will give an extra shape anisotropy. At high temperature, the anisotropy is parallel and, at low temperature, the angle decreases only around 60° due to the counterbalancing of the interface anisotropy (30° due to PMA and RMA) by the volume anisotropy due to pure amorphous iron and terbium (90°) in the center of Fe and Tb layers.

For t_{Tb}=1.9 nm and t_{Fe}=2.7 nm, x-ray diffraction and Mössbauer results show that pure iron is crystallized and this can be compared to the previous behavior. Here the volume anisotropy of pure amorphous iron is replaced by a stronger magnetocrystalline anisotropy of bcc α-Fe. When the temperature decreases, the interface anisotropy increases, as previously, but the β angle decreases more slowly because of the higher anisotropy of crystalline α-Fe.

To our knowledge, there has been no previous systematic Mössbauer study of the magnetic anisotropy in amorphous Tb/Fe multilayers. Some studies have been devoted to evaporated multilayers with higher iron thickness, where Fe layers are crystallized.[6,39,43] A reorientation can also be observed, as in our last sample with crystalline iron. The results in the literature are not consistent. Sajieddine *et al.*[43] found a behavior in rough agreement with our results, i.e., the influence of Fe and Tb thicknesses on the β angle at low temperature. However, Scholz *et al.*[6] and Mibu *et al.*[39] found a β angle at low temperature independent of t_{Fe} or t_{Tb} and always in the 30°–40° range. These surprising differences could be attributed to different preparative elaborations, leading to structural differences, such as the spread of the interfaces, which governs the strength of the perpendicular anisotropy. Some authors intended to modelize the temperature dependence of the anisotropy.[11,44,45] In fact, these models take into account only a part of the interactions and it would be interesting to develop a more complete model.

VII. CONCLUSION

We have presented the first systematic structural and magnetic study of Tb/Fe multilayers in the amorphous range, i.e., in the range where the thicknesses of the layers are small. It

is to be noted that this is the domain which is of industrial interest, because it is the range of perpendicular magnetic anisotropy. For low t_{Fe} and t_{Tb} thicknesses, all results show a compositionally modulated interface with magnetic properties (T_c) very close to the Fe-Tb amorphous alloys of the same global composition. When t_{Fe} or t_{Tb} is sufficient, a pure amorphous iron or terbium phase appears in the center of the layers. In our samples, pure amorphous Fe appears from t_{Fe} close to 1.2 nm and interface spreads on about 2(Tb+Fe) layers. The pure amorphous iron layer gives specific magnetic properties (T_c, magnetic anisotropy). In particular, at room temperature, when it is paramagnetic, it contributes to the reduction of magnetic interactions. All magnetic experimental results are interpreted consistently in agreement with the structure.

ACKNOWLEDGMENTS

The authors would like to thank P. Veillet for help in magnetization measurements which were performed in the Institut d'Electronique Fondamentale at Orsay (URA CNRS 022, France). This work was supported by the French Ministère de la Recherche et de la Technologie under the MRT Contract No. 92S0151.

[1] N. Sato, J. Appl. Phys. **59**, 2514 (1986).
[2] K. Yamauchi, K. Habu, and N. Sato, J. Appl. Phys. **64**, 5748 (1988).
[3] K. Cherifi, P. Donovan, C. Dufour, Ph. Mangin, and G. Marchal, Phys. Status Solidi A **122**, 311 (1990).
[4] Z. S. Shan and D. J. Sellmyer, Phys. Rev. B **42**, 10 433 (1990).
[5] S. Honda, T. Kimura, M. Nawate, and T. Kusuda, J. Magn. Soc. Jpn. **15**, S-1 61 (1991).
[6] B. Scholz, R. A. Brand, and W. Keune, J. Magn. Magn. Mater. **104-107**, 1889 (1992).
[7] S. Honda, T. Kimura, and M. Nawate, J. Magn. Magn. Mater. **121**, 116 (1993).
[8] F. Richomme, A. Fnidiki, P. Auric, J. Teillet, P. Boher, and Ph. Houdy, Hyperfine Interact. **92**, 1243 (1994).
[9] B. Scholz, R. A. Brand, and W. Keune, Phys. Rev. B **50**, 2537 (1994).
[10] L. T. Baczewski, M. Piecuch, J. Durand, G. Marchal, and P. Delcroix, Phys. Rev. B **40**, 11 237 (1989).
[11] Z. S. Shan, D. J. Sellmyer, S. S. Jaswal, Y. J. Wang, and J. X. Shen, Phys. Rev. B **42**, 10 446 (1990).
[12] K. Mibu, N. Hosoito, and T. Shinjo, Hyperfine Interact. **68**, 341 (1991).
[13] C. Dufour, K. Cherifi, A. Bruson, G. Marchal, and Ph. Mangin, Phys. Status Solidi A **125**, 561 (1991).
[14] B. Scholz, R. A. Brand, W. Keune, U. Kirschbaum, E. F. Wassermann, K. Mibu, and T. Shinjo, J. Magn. Magn. Mater. **93**, 499 (1991).
[15] J. Teillet, A. Fnidiki, F. Richomme, P. Boher, and Ph. Houdy, J. Magn. Magn. Mater. **123**, 359 (1993).
[16] J. Teillet and F. Varret, MOSFIT program (unpublished).
[17] F. Varret, in *Proceedings of International Conference on the Applications of the Mössbauer Effect* (Indian National Science Academy, New Delhi, 1982), p. 129.
[18] G. S. Cargill, in Magnetism and Magnetic Materials, edited by C. D. Graham and J. J. Rhyne, AIP Conf. Proc. No. 18 (AIP, New York, 1973), p. 631.
[19] K. Fukuda, S. Katayama, T. Katayama, A. Nukui, and A. Makisima, Jpn. J. Appl. Phys. **25**, 1640 (1986).
[20] M. Tewes, J. Sweck, and H. Hoffmann, J. Magn. Magn. Mater. **95**, 43 (1991); J. Phys. Condens. Matter **6**, 835 (1994).
[21] F. Pierre, P. Boher, H. Kergoat, Ph. Houdy, J. Ferre, and G. Penissard, J. Appl. Phys. **69**, 4565 (1991).
[22] R. Krishnan and F. Machizaud, Mater. Sci. Eng. B **6**, 257 (1990).
[23] M. J. Kim, J. S. Bow, L. W. Carpenter, J. Liu, S. J. Kim, S. K. Lee, W. M. Kim, and J. S. Yoon, IEEE Trans. Magn. **30**, 4398 (1994).
[24] K. Cherifi, C. Dufour, M. Piecuch, A. Bruson, Ph. Bauer, G. Marchal, and Ph. Mangin, J. Magn. Magn. Mater. **93**, 609 (1991).
[25] N. Sato and K. Habu, J. Appl. Phys. **61**, 4287 (1987).
[26] Z. S. Shan and D. J. Sellmyer, J. Appl. Phys. **67**, 5713 (1990).
[27] G. Endl, B. Bielmeier, and H. Hoffmann (unpublished).
[28] Z. S. Shan, D. J. Sellmyer, S. S. Jaswal, Y. J. Wang, and J. X. Shen, Phys. Rev. Lett. **63**, 449 (1989).
[29] F. Richomme, B. Scholz, R. A. Brand, W. Keune, and J. Teillet, J. Magn. Magn. Mater. (to be published).
[30] H. A. Alperin, J. R. Cullen, and A. E. Clark, in *Magnetism and Magnetic Materials*, edited by J. J. Becker, G. H. Lander, J. J. Rhyne, AIP. Conf. Proc. No. 29 (AIP, New York, 1976), p. 186.
[31] J. J. Rhyne, IEEE Trans. Magn. **MAG-21**, 1990 (1985).
[32] V. S. Rusakov, B. S. Vvedensky, E. T. Voropaeva, and E. N. Nikolaev, IEEE. Trans. Magn. **28-2**, 2524 (1992).
[33] Y. Mimura, N. Imamura, and T. Kobayashi, IEEE Trans. Magn. **MAG-12**, 779 (1976); Y. Mimura, N. Imamura, T. Kobayashi, A. Okada, and Y. Kushiro, J. Appl. Phys. **49**, 1208 (1978).
[34] J. W. M. Biesterbos, J. Phys. (Paris) Colloq. **40**, CS-274 (1979).
[35] G. Bayreuther, D. Hoffmann, M. Haidl, and C. Reuter (unpublished).
[36] K. Handrich, Phys. Status Solidi **32**, 55 (1969).
[37] P. Hansen, C. Clausen, B. Much, M. Rosenkranz, and K. Witter, J. Appl. Phys. **66**, 756 (1989).
[38] V. S. Rusakov, B. S. Vvedensky, S. N. Gadetsky, E. T. Voropaeva, V. V. Kochetov, A. V. Stupnov, and E. N. Nikolaev, J. Magn. Soc. Jpn. **17-S1**, 35 (1993).
[39] K. Mibu, N. Hosoito, and T. Shinjo, J. Magn. Magn. Mater. **126**, 343 (1993).
[40] J. J. Rhyne, S. J. Pickart, and H. A. Alperin, Phys. Rev. Lett. **29**, 1562 (1972).
[41] R. Harris, M. Plischke, and M. J. Zuckermann, Phys. Rev. B **31**, 160 (1973).
[42] B. Dieny, R. Ribas, and B. Barbara, J. Magn. Magn. Mater. **130**, 189 (1994).
[43] M. Sajieddine, Ph. Bauer, C. Dufour, K. Cherifi, G. Marchal, and Ph. Mangin, J. Magn. Magn. Mater. **113**, 243 (1992).
[44] Y. J. Wang and W. Kleeman, Phys. Rev. B **44**, 5132 (1991).
[45] A. Moschel and K. Usadel, Phys. Rev. B **49**, 12 868 (1994).